Journal of Organometallic Chemistry 696 (2011) 179–187

Contents lists available at ScienceDirect

Journal of Organometallic Chemistry

journal homepage: www.elsevier.com/locate/jorganchem

Palladium(II) 3-iminophosphine (3IP) complexes: Active precatalysts for the intermolecular hydroamination of 1,2-dienes (allenes) and 1,3-dienes with aliphatic amines under mild conditions

Glenn Kuchenbeiser, Andrew R. Shaffer, Nicholas C. Zingales, John F. Beck, Joseph A.R. Schmidt*

Department of Chemistry, The University of Toledo, 2801 W. Bancroft St. MS 602, Toledo, OH 43606 3390, USA

ARTICLE INFO

Article history:
Received 19 July 2010
Received in revised form
23 August 2010
Accepted 24 August 2010
Available online 1 October 2010

Keywords:
Hydroamination
Allenes
Butadienes
Palladium
Iminophosphines
Catalysis

ABSTRACT

The synthesis of alicyclic 3-iminophosphine ligands is extended to include a new framework incorporating a cyclohexenyl backbone with an *N*-aryl imino functionality (**3IP^{Ar}**). Accordingly, a series of palladium(II) complexes employing this new ligand have been synthesized and utilized in the intermolecular hydroamination of 3-methyl-1,2-butadiene (1,1-dimethylallene) and 2,3-dimethyl-1,3-butadiene with secondary amines. The complex **[(3IP^{Ar})Pd(allyl)]OTf** displays excellent catalytic activity in these reactions, selectively producing allylic amine products in high conversion under mild conditions, with an improved rate relative to that observed for our previously reported catalysts. Further, the reactivity trends for the (3IP)Pd triflate systems prove to be complimentary to other known late transition metal based catalytic systems.

1. Introduction

The formation of C–N bonds is essential to the synthesis of a wide variety of pharmaceutically and industrially important nitrogen containing organic molecules [1,2]. Although there are a number of reliable methods for making these bonds, by far the most atom-efficient routes involve the direct addition of N–H across unsaturated C–C bonds, a process known as hydroamination [3–10]. A variety of late transition metal catalyzed *intra*molecular variants of this reaction have been reported, allowing the formation of nitrogen containing heterocycles [11–32]. For obvious entropic reasons, *inter*molecular hydroamination has proven to be more challenging, especially with unactivated alkenes, and so the discovery of new catalysts effecting this reaction remains a very active topic of research.

Recently Bertrand and co-workers reported the catalytic intermolecular Markovnikov hydroamination of allenes with primary and secondary amines, as well as ammonia, utilizing a cationic gold–carbene complex [33,34]. Additionally, the Widenhoefer group has shown similar reactivity using a gold-phosphine/AgOTf system [35] and other gold-based systems [36–39]. While these systems display excellent activity, in both cases elevated reaction temperatures (between 70 and 130 °C) were required, and the cost of gold precursors is non-trivial. Clearly, the discovery of more mild catalytic methodologies would be advantageous.

Previously, we reported a series of 3-iminophosphine (3IP) palladium(II) complexes that display hemilabile behavior (Fig. 1) [40,41]. One of these complexes, the triflate salt of [(3IP)Pd(allyl)]$^+$, was shown to have moderate catalytic activity for the intermolecular hydroamination reactions of 1,3-cyclohexadiene and phenylacetylene with primary and secondary amines to yield enamines and imines without the need for an acid co-catalyst [41]. Expanding on these previous results, we now report the synthesis of a new 3IP framework containing a cyclohexenyl alicyclic backbone with *N*-aryl substituted imine and have found that the corresponding (3IP^{Ar})Pd triflates are active precatalysts in the intermolecular hydroamination of acyclic 1,2- and 1,3-dienes giving high conversion to allylic amine products under mild conditions.

2. Results and discussion

2.1. Synthesis and characterization

The modular and general methodology used for the synthesis of the 3-iminophosphine (3IP) ligand framework allows a great deal of flexibility with regards to both steric and electronic parameters

* Corresponding author. Tel.: +1 419 530 1512; fax: +1 419 530 4033.
E-mail address: Joseph.Schmidt@utoledo.edu (J.A.R. Schmidt).

0022-328X/$ – see front matter © 2010 Elsevier B.V. All rights reserved.
doi:10.1016/j.jorganchem.2010.08.033

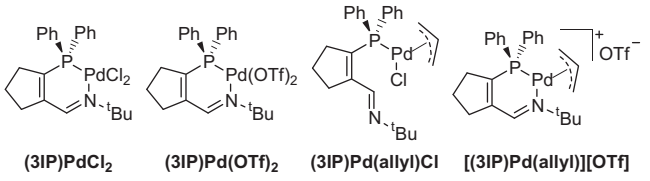

Fig. 1. Previously reported 3IP–palladium complexes tested in this study (OTf = CF_3SO_3).

available for complexation to a transition metal center. With this in mind, we sought to synthesize a new 3IP ligand and its corresponding Pd complexes in order to explore the effect of altered substituents on catalytic efficiency in hydroamination reactions. Specifically, substitution of the imine nitrogen with an aryl rather than an alkyl group was anticipated to yield weaker coordination to a metal center, while 2,6-disubstitution of the aryl ring should encourage imine lability due to increased projection of steric bulk towards the metal center. We expected the combination of these features to allow for better access to a vacant coordination site for catalysis.

The 3-iminophosphine ligand system (**3IP^{Ar}**) used in this study was synthesized in excellent yield using a sequence analogous to that reported in our earlier work (Scheme 1) [41]. Treatment of commercially available cyclohexanone with the Vilsmeier-Haack reagent and subsequent workup gave an alicyclic α,β-unsaturated, β-chloroaldehyde in 90% yield as a red liquid (intermediate **a**; Scheme 1). Schiff base condensation using 2,6-dimethylaniline at 0 °C provided the corresponding β-chloroimine (intermediate **b**) as a red oil in 96% yield. The ligand synthesis was completed by reaction with lithium diphenylphosphide in toluene at −78 °C to afford an off-white solid in 88% yield. ^{31}P NMR spectroscopy revealed a distinctive signal at −12.6 ppm, while the ^{1}H NMR spectrum displayed a characteristic doublet for the imine proton at 9.05 ppm ($^{4}J_{PH}$ = 9.0 Hz).

In order to examine the coordination chemistry of **3IP^{Ar}**, and for comparison with our previously reported **3IP** complexes, we began with the classical precursor $PdCl_2$ (Scheme 2). Addition of a solution of **3IP^{Ar}** in methylene chloride to a slurry of $PdCl_2$ in acetonitrile, stirring overnight and subsequent workup resulted in a yellow powder in 60% yield. The new compound was identified spectroscopically as the desired species **(3IP^{Ar})PdCl$_2$**. Room temperature ^{31}P NMR spectroscopy of this compound in $CDCl_3$ shows a singlet at 30.3 ppm, shifted significantly downfield from that for the free ligand (−12.6 ppm), while the ^{1}H and ^{13}C NMR spectra are analogous to our previously reported **(3IP)PdCl$_2$**. The imine proton resonance shifts significantly upfield to 7.46 ppm in **(3IP^{Ar})PdCl$_2$**, consistent with coordination of the nitrogen atom to the palladium center. Single crystals suitable for an X-ray diffraction study were obtained by slow evaporation of a chloroform solution, confirming the proposed κ^2 coordination mode (Fig. 2). In the solid state, the complex has a distorted square planar geometry with a ligand bite angle of 88.6° and a significant folding of the ligand to give a boat-like conformation. This overall shape and the structural parameters

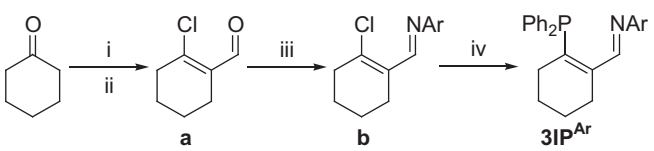

Scheme 1. Synthesis of alicyclic (cyclohexenyl) **3IP^{Ar}** ligand (Ar = 2,6-$Me_2C_6H_3$). Legend: (i) $POCl_3$, DMF, 0 °C, 30 min; (ii) ice, $NaHCO_3$; (iii) $H_2N(2,6\text{-}Me_2C_6H_3)$, Et_2O, 0 °C, 14 h; (iv) Ph_2PLi, toluene, −78 °C, 14 h.

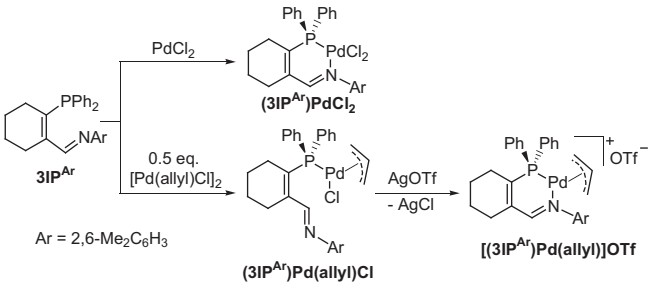

Scheme 2. Synthesis of *N*-aryl-3-iminophosphine palladium complexes.

of **(3IP^{Ar})PdCl$_2$** are very similar to that reported for **(3IP)PdCl$_2$** [41] with all of the notable bond lengths being nearly equal between the two complexes (Table 1). The main differences in the observed metrical parameters involve the bond angles associated with the ligand backbone, which are likely an effect of the different ring sizes within the alkenyl ligand framework.

We next sought to synthesize the **3IP^{Ar}** analog of our reported hydroamination catalyst: **[(3IP)Pd(allyl)]OTf** [41]. Combining room temperature methylene chloride solutions of **3IP^{Ar}** and [Pd(allyl)Cl]$_2$, stirring overnight, and subsequent workup gave a yellow microcrystalline solid in 95% yield. The ^{31}P NMR spectrum of a room temperature $CDCl_3$ solution of this material shows a singlet at 19.1 ppm, shifted downfield from the free ligand by nearly 32 ppm and similar to that of the corresponding **3IP** analog. Notable features of the ^{1}H NMR spectrum include a doublet at 8.81 ppm ($^{4}J_{PH}$ = 3.6 Hz) for the imine proton resonance and the equivalency of aryl-methyl resonances at 1.88 ppm, indicating a κ^1 coordination mode. Additional data from ^{13}C NMR spectroscopy and high resolution mass spectrometry confirmed the identity of the product as **(3IP^{Ar})Pd(allyl)Cl**.

Halogen abstraction from **(3IP^{Ar})Pd(allyl)Cl** with silver triflate in methylene chloride and subsequent workup gave a new yellow solid in 88% yield. The room temperature ^{31}P NMR spectrum in $CDCl_3$ revealed a single resonance at 25.2 ppm, further downfield shifted from both the precursor and free ligand. As in the case of **(3IP^{Ar})PdCl$_2$**, the ^{1}H NMR signal for the imine proton was found significantly upfield (7.70 ppm) from that of free ligand (**3IP^{Ar}**: 9.05 ppm) or the precursor complex (**(3IP)Pd(allyl)Cl**: 8.81 ppm), consistent with a κ^2 coordination mode. This analysis was confirmed by the presence of two singlets at 2.06 and 1.95 ppm, corresponding to inequivalent aryl-methyl groups due to hindered rotation of the *N*-aryl ring in the **[(3IP^{Ar})Pd(allyl)]OTf** complex. X-ray quality crystals were grown by slow diffusion of pentane into a THF solution of this complex. The crystal structure of **[(3IP^{Ar})Pd(allyl)]OTf** confirmed the κ^2 coordination mode in this complex (Fig. 3). In a similar fashion to that observed for **[(3IP)Pd(allyl)]PF$_6$** [40] the allyl group was disordered as a 4:1 ratio of the *cis* and *trans* isomers, while the two distal carbon atoms of the cyclohexenyl ring were disordered in a nearly 1:1 ratio of two different boat-like conformations. Surprisingly, an examination of the bond lengths in this complex revealed *stronger* bonding of the imine nitrogen to the palladium center, as noted by the significantly shorter Pd1–N1 bond length in **[(3IP^{Ar})Pd(allyl)]OTf** than was observed in the previous **[(3IP)Pd(allyl)]OTf** complex (Table 1). All of the other notable bond lengths were found to be quite similar for the two complexes. Significant differences in the bond angles were also observed, with the ligand bite angle for the **(3IP^{Ar})** complex found to be almost ideal at 90.44(6) degrees. The various differences in bond angles are most likely the result of the cyclohexenyl backbone in this new complex, relative to the cyclopentenyl backbone of the previously reported 3IP complex. In fact, the shorter

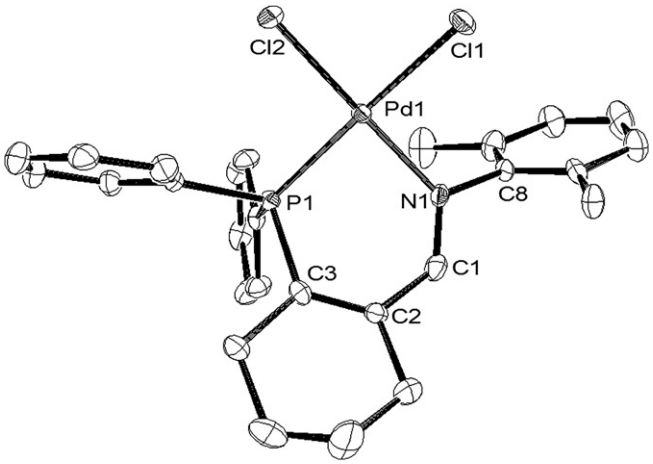

Fig. 2. ORTEP diagram (50% thermal ellipsoids) of **(3IP^{Ar})PdCl$_2$**. Hydrogen atoms and two chloroform solvent molecules omitted for clarity.

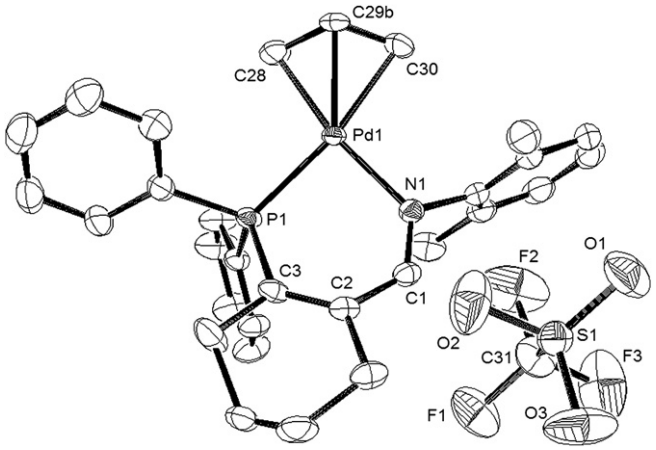

Fig. 3. ORTEP diagram (50% thermal ellipsoids) of **[(3IP^{Ar})Pd(allyl)]OTf**. Hydrogen atoms, three disordered carbon atoms and THF solvent molecule omitted for clarity.

Pd1–N1 bond length may also reflect changes caused by the different backbone unit, as it may now have less ring strain than was originally observed in the initial report. Clearly, the study of further ligand derivatives is necessary to fully delineate the effects of imine substituent and backbone composition.

2.2. Catalysis

While moderate success was achieved in the hydroamination of both phenylacetylene and 1,3-cyclohexadiene using **[(3IP)Pd(allyl)]OTf**, these results were limited by competing cyclotrimerization and aromatization reactions, as evidenced by the formation of aryl side products and the need for a large excess of diene/alkyne present [41]. Therefore, it was preferable to explore substrates not plagued by these competitive pathways. 1,2-Dienes (allenes) constitute an important class of unsaturated substrates that have recently been shown to undergo hydroamination via cationic transition metal catalysts [33,42] so we postulated that our cationic 3IP-palladium systems may display similar catalytic activity for allene hydroamination. Preliminary screening was performed using 5 mol% of **[(3IP^{Ar})Pd(allyl)]OTf** at room temperature with 3-methyl-1,2-butadiene and morpholine as reactants. Upon monitoring the reaction progress by ^{1}H NMR spectroscopy in deuterated benzene, we observed the formation of a new set of resonances consistent with a branched hydroamination product **1a**, as well as a second set of resonances corresponding to the linear olefin product **2a**, in a ratio of ca. 2:1 with a total conversion of 91% within 30 min. Within 4 h, the reaction proceeded with complete regioselectivity, quantitatively forming the allylic amine product **2a**, afforded via isomerization of the kinetic branched product (Table 2, entry 12). Reduction of the catalyst loading to 1 mol% also gave quantitative conversion to **2a**, but at a five fold increase in reaction time. To the best of our knowledge, this is the first example of room temperature hydroamination of allenes with dialkylamines using a late transition metal catalyst.

Although all of our 3IP and 3IP^{Ar} Pd triflates were found to be competent hydroamination catalysts at 5 mol% loading, the best reaction rate was obtained using **[(3IP^{Ar})Pd(allyl)]OTf** (Table 2, entries 10–13). As expected, the various corresponding (3IP)Pd chloride complexes showed no activity, even at extended reaction times, higher temperatures, or with the addition of silver triflate (Table 2, entries 4–9). The detrimental effect of chloride ions is

Table 1
Selected bond distances (Å) and angles (deg) in crystal structures[a].

	(3IP)PdCl$_2$	(3IP^{Ar})PdCl$_2$	[(3IP)Pd(allyl)]OTf	[(3IP^{Ar})Pd(allyl)]OTf
Pd1–P1	2.226(1)	2.220(1)	2.267(5)	2.2597(6)
Pd1–N1	2.065(4)	2.054(4)	2.141(3)	2.080(2)
Pd1–Cl^P	2.396(1)	2.362(1)	–	–
Pd1–Cl^N	2.298(1)	2.289(1)	–	–
Pd1–C^P	–	–	2.238(5)	2.210(2)
Pd1–C^N	–	–	2.102(4)	2.110(2)
P1–C3	1.804(4)	1.817(5)	1.81(1)	1.826(2)
N1–C1	1.285(6)	1.278(6)	1.284(1)	1.283(3)
C1–C2	1.463(6)	1.478(6)	1.465(4)	1.476(3)
C2–C3	1.351(6)	1.343(6)	1.342(3)	1.347(3)
P1–Pd1–N1	85.3(7)	88.6(1)	92.9(5)	90.44(6)
Pd1–P1–C3	100.2(2)	108.2(1)	105.6(9)	111.45(7)
Pd1–N1–C1	123.1(2)	126.5(3)	123.5(8)	129.7(2)
N1–C1–C2	123.6(2)	128.7(4)	127.8(9)	128.5(2)
C1–C2–C3	124.1(9)	124.1(4)	129.8(2)	126.9(2)

[a] Superscripted letters indicate the atom positioned trans to the denoted atom. Data for **3IP** complexes reproduced from Ref. [41].

Table 2
Hydroamination of 3-methyl-1,2-butadiene with morpholine[a].

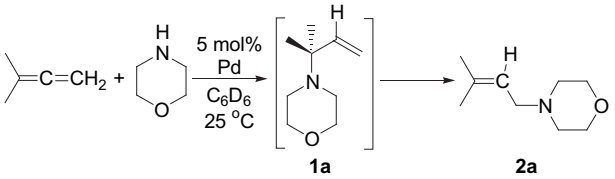

Entry	Precatalyst	Time (h)	Conversion (%)[b]
1	$PdCl_2$	48	none
2	$[Pd(allyl)Cl]_2$	48	none
3	$[Pd(allyl)Cl]_2$ + 2 AgOTf	48	none
4	**(3IP)PdCl$_2$**	48	none
5	**(3IP^{Ar})PdCl$_2$**	48	none
6	**(3IP)PdCl$_2$** + 2 AgOTf	48	none
7	**(3IP^{Ar})PdCl$_2$** + 2 AgOTf	48	none
8	**(3IP)Pd(allyl)Cl**	48	none
9	**(3IP^{Ar})Pd(allyl)Cl**	48	none
10	**[(3IP)Pd(allyl)]OTf**	4	45 (**1a**) + 44 (**2a**)
11	**[(3IP)Pd(allyl)]OTf**	20	>98 (**2a**)
12	**[(3IP^{Ar})Pd(allyl)]OTf**	4	>98 (**2a**)
13	**(3IP)Pd(OTf)$_2$**	20	>98 (**2a**)
14	**[(3IP^{Ar})Pd(allyl)]OTf** + NEt_3	24	70 (**2a**)
15	**[(3IP^{Ar})Pd(allyl)]OTf** + HBF_4	4	97 (**2a**)

[a] Conditions: 0.32 mmol allene, 0.32 mmol morpholine, 0.5 mL C_6D_6, 25 °C, sealed NMR tube.
[b] Conversion determined by ^{1}H NMR spectroscopy.

consistent with other reports in the literature [43]. The addition of 1 eq. of a strong acid ($HBF_4 \cdot OEt_2$) proved to have no effect on reaction rate or conversion, while the addition of an amine base (triethylamine) slowed the catalysis such that product formation was reduced to 70% after 24 h (Table 2, entries 14–15). This result is consistent with competitive inhibition at the metal center and perhaps explains the significant decrease in rate over time observed for all of our catalyses, as tertiary amine bases constitute the hydroamination reaction products. Additionally, control experiments using silver triflate, palladium allyl chloride dimer, palladium(II) chloride, or their mixtures resulted in no conversion to hydroamination products (Table 2, entries 1–3), indicating the necessity of the preformed 3IP–Pd triflate complexes in order to achieve catalysis. Solvent screening revealed that non-polar, aromatic solvents such as benzene and toluene afforded the highest conversions, while reactions performed in either acetonitrile or chloroform displayed reduced catalytic efficiency (Table 3, entries 1–4). Furthermore, the presence of significant amounts of a donor solvent (THF) did not significantly decrease the catalytic efficiency (Table 3, entry 5).

Using our optimized conditions, we examined the scope of secondary amines amenable to the hydroamination of 3-methyl-1,2-butadiene using 5 mol% **[(3IP^{Ar})Pd(allyl)]OTf** as catalyst (Table 4). Both cyclic and acyclic dialkylamines were the best substrates for this reaction, with each giving quantitative conversion to the linear products at room temperature in less than 6 h (Table 4, entries 1–12). Exceptions to this occurred only for the bulky substrates 2,2,6,6-tetramethylpiperidine and diisopropylamine. In general, cyclic *N*-aryl-alkylamines proved to be more challenging substrates (Table 4, entries 13–15). For example, the reaction with indoline gave a quantitative conversion at room temperature but required 24 h. Moreover, reactions involving the bulkier 2-methylindoline or 1,2,3,4-tetrahydroquinoline gave only poor to moderate results and required elevated temperatures and long reaction times. Lastly, all attempts at hydroamination using *N*-methyl aniline resulted in the rapid formation of Pd black without any detectable hydroamination products. So, overall the reactivity trend for the **[(3IP^{Ar})Pd(allyl)]OTf** catalytic system appears to favor more basic amines, in stark contrast with other known catalysts that have more success with the less basic amines [33,35,43]. Additionally, hydroamination product isolation was straightforward with excellent recovery (>80%) of the amines produced.

Conjugated dienes constitute another class of unsaturated substrates of interest for intermolecular hydroamination. These reactions typically result in the formation of mixtures of telomerization products, with 1:1 adducts formed in variable yields depending upon the substrate and catalyst employed [4,44]. A notable exception is found in the work of Yoshifuji employing a diphosphinidenecyclobutane Pd catalyst, where the reaction of aniline with various conjugated dienes selectively gave high yields of the desired allylic amine products, although the scope of amine substrates was not explored [45]. Given our success in the intermolecular hydroamination of 3-methyl-1,2-butadiene, we also chose to examine hydroamination of the commercially available 2,3-dimethyl-1,3-butadiene. Although this substrate proved to be more challenging than dimethylallene, requiring heating at 60 °C for 24 h or more depending on the amine employed, allylic amine products were obtained for a variety of amines. While primary amines showed no conversion, secondary dialkylamines readily

Table 3
Effect of solvent on Pd catalyzed hydroamination of 3-methyl-1,2-butadiene with morpholine[a].

Entry	Solvent	Conversion (%)[b]
1	Benzene	>98
2	Toluene	>98
3	Acetonitrile	48
4	Chloroform	12
5	Benzene/THF (1:1)	>98

[a] Conditions: 0.32 mmol allene, 0.32 mmol morpholine, 5 mol% **[(3IP^{Ar})Pd(allyl)]OTf**, 0.5 mL solvent, 25 °C, 24 h, sealed NMR tube.
[b] Conversion determined by ^{1}H NMR spectroscopy.

Table 4
Catalytic hydroamination of 3-methyl-1,2-butadiene with secondary amines using **[(3IP^{Ar})Pd(allyl)]OTf** [a].

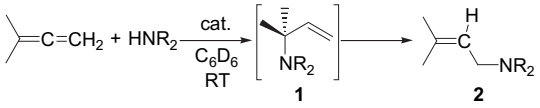

Entry	Amine	Time (hrs)	Product	Conversion (%)[b]
1		4	**2a**	>98
2	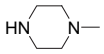	<1	**2b**	>98
3		3	**2c**	>98
4		6	**2d**	>98
5		6	**2e**	>98
6	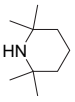	48	–	–
7	$HNEt_2$	3	**2f**	>98
8	HN^nBu_2	3	**2g**	>98
9	HN^iPr_2	48	–	–
10	HN(Me)(^{n}Bu)	4	**2h**	>98
11	$HN(CH_2Ph)_2$	30	**2i**	>98[c]
12	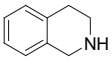	3	**2j**	>98
13		24	**2k**	>98
14	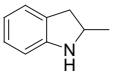	24(96)	**2l**	28(55)[d,e]
15		24(96)	**2m**	11(25)[d,e]
16	HN(Me)(Ph)	48	–	–[f]

[a] Conditions: 0.32 mmol allene, 0.32 mmol amine, 5 mol% **[(3IP^{Ar})Pd(allyl)]OTf**, 0.5 mL C_6D_6, 25 °C, sealed NMR tube.
[b] Conversion measured by ^{1}H NMR spectroscopy.
[c] Reaction at 50 °C.
[d] Reaction at 90 °C.
[e] Conversion in parenthesis after 4 d.
[f] Pd black rapidly formed.

underwent 1,4-addition to afford the corresponding tertiary allylic amine products (Table 5). The best results were obtained for cyclic secondary amines, such as morpholine and piperidine (Table 5, entries 1–5). Non-cyclic secondary amines provided moderate conversion at best, while the bulkier substrates showed little or no reactivity at all (Table 5, entries 6–9). Cyclic *N*-aryl-alkylamines were again quite sluggish with only indoline providing notable conversion after a 72 h reaction period (Table 5, entry 11). In general, the hydroamination of 2,3-dimethyl-1,3-butadiene with secondary amines provided only moderate product formation and required long reaction times, limiting the utility of the **[(3IP^{Ar})Pd(allyl)]OTf** catalyst for reactions with this substrate.

3. Conclusions

The synthesis of a new alicyclic 3-iminophosphine ligand has been achieved with the formation of a cyclohexenyl based *N*-aryl imino 3IP ligand (**3IP^{Ar}**). Reactions with Pd precursors yielded a variety of **3IP^{Ar}** palladium(II) complexes whose spectroscopic and structural parameters matched well with the corresponding previously reported (3IP)Pd species. Despite the ligand similarities, the **3IP^{Ar}** catalytic system shows increased catalytic activity in the intermolecular hydroamination of 1,2- and 1,3-dienes relative to its **3IP** counterparts. Based on the differences observed by comparison of the catalyst crystal structures, this improved reactivity seems to be caused by the larger backbone alicyclic ring, although we can not rule out the effect of changes to the imine basicity or increased imine steric interactions leading to greater lability and therefore a more accessible vacant site at the Pd center. The reactivity trends for these systems are complimentary to other known late transition metal based catalytic systems with highly basic secondary dialkylamines proving to be the best substrates, leading to quantitative conversion to allylamine products within hours at room temperature. Further exploration of ligand parameters for our 3IP systems and their effect on catalytic activity are currently underway.

Table 5
Catalytic hydroamination of 2,3-dimethyl-1,3-butadiene with secondary amines using **[(3IP^{Ar})Pd(allyl)]OTf** [a].

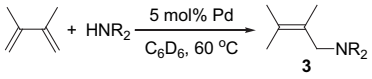

Entry	Amine	Product	Conversion (%)[b]
1		**3a**	89
2	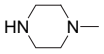	**3b**	38(49)[c]
3		**3c**	49
4		**3d**	85
5		**3e**	40(56)[c]
6	$HNEt_2$	**3f**	38(55)[c]
7	HN^nBu_2	**3g**	15(36)[c]
8	HN^iPr_2	–	–
9	$HN(CH_2Ph)_2$	–	<5
10	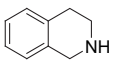	**3j**	69(87)[c]
11		**3k**	18(74)[c]

[a] Conditions: 0.32 mmol diene, 0.32 mmol amine, 5 mol% **[(3IP^{Ar})Pd(allyl)]OTf**, 0.5 mL C_6D_6, 60 °C, 24 h, sealed NMR tube.
[b] Conversion determined by ^{1}H NMR spectroscopy.
[c] Number in parenthesis represents conversion after 72 h; percentage continues to increase with longer reaction times.

4. Experimental

4.1. General considerations

Intermediates **a** and **b** were synthesized under ambient atmosphere. All other reactions were performed using standard Schlenk and drybox techniques. *n*-Butyllithium (1.6 M in hexanes), palladium(II) chloride, (allyl)palladium(II) chloride dimer, chlorodiphenylphosphine, and silver triflate were purchased from Strem and used without further purification. $CDCl_3$ and C_6D_6 were purchased from Cambridge Isotope Laboratories and vacuum transferred from CaH_2 and Na/benzophenone ketyl, respectively. Pentane, tetrahydrofuran, and methylene chloride were purified by passage through a column of activated 4 Å molecular sieves and degassed with nitrogen prior to use. Diethyl ether and toluene were purified by passage through a column of activated alumina and a column of activated 4 Å molecular sieves and degassed with nitrogen prior to use. Acetonitrile and chloroform were purified by vacuum transfer from CaH_2. Cyclohexanone, $POCl_3$, *N*,*N*-dimethylformamide, sodium, 3-methyl-1,2-butadiene, 2,3-dimethyl-1,3-butadiene, and all amines were purchased from commercial vendors. All amines used for hydroamination were dried by vacuum transfer from $CaH_2 \cdot LiPPh_2$ [41], **(3IP)PdCl$_2$** [41], **(3IP)Pd(allyl)Cl** [41], **[(3IP)Pd(allyl)]OTf** [41], and **(3IP)Pd(OTf)$_2$** [40] were synthesized as previously reported. NMR data were obtained on Inova 600 or 400 MHz or Gemini 200 MHz spectrometers at ambient temperature. NMR chemical shifts are given relative to residual solvent peaks and were taken in $CDCl_3$, unless otherwise noted. ^{31}P and ^{19}F NMR spectra were externally referenced to 0.00 ppm with 5% H_3PO_4 in D_2O and $CFCl_3$, respectively. IR samples were prepared as Nujol mulls or neat films and taken between KBr plates on a Perkin–Elmer XTL FTIR spectrophotometer. Melting points were observed on a Mel-Temp apparatus in sealed capillary tubes and are uncorrected. Elemental analyses were determined by Desert Analytics, Tucson, AZ and Galbraith Laboratories, Knoxville, TN. High resolution mass spectrometry analysis was performed by the University of Illinois Mass Spectrometry Laboratory, Urbana, IL. X-ray structure determinations were performed at the Ohio Crystallographic Consortium housed at The University of Toledo.

4.2. Catalyst synthesis

4.2.1. β-Chloroaldehyde intermediate (a)

The procedure was modified from Benson and Pohland [46]. Phosphorus oxychloride (6.53 g, 42.6 mmol) was added to a flask containing *N*,*N*-dimethylformamide (3.89 g, 53.2 mmol) in an ice bath and stirred for 7 min. The ice bath was replaced with an ambient temperature water bath and stirred for an additional 8 min. The mixture was cooled to 0 °C and cyclohexanone (2.61 g,

26.6 mmol) was added and stirred for 15 min. The ice bath was replaced with an ambient temperature water bath and stirred for an additional 15 min. The orange solution was poured into an Erlenmeyer flask containing ice (150 g) and made basic by addition of sodium bicarbonate. After extraction with diethyl ether (3 × 100 mL), the combined organic extracts were washed with 100 mL of a saturated aqueous sodium bicarbonate solution, 100 mL of brine, and water (3 × 100 mL). The organic layer was dried with magnesium sulfate for 20 min, filtered, and the volatiles removed in vacuo to yield a red liquid, which was used without further purification (3.47 g, 90.2%); ^{1}H NMR δ = 10.19 (s, 1H), 2.59–2.56 (m, 2H), 2.29–2.26 (m, 2H), 1.78–1.74 (m, 2H), 1.67–1.63 (m, 2H); ^{13}C{^{1}H} NMR δ = 191.5, 151.7, 133.7, 36.1, 24.0, 23.4, 21.3; IR(neat) 3330 (w), 2932 (s), 2848 (m), 2744 (w), 2660 (w), 2356 (w), 2324 (w), 1675 (s), 1618 (s), 1450 (w), 1434 (m), 1345 (m), 1266 (w), 1214 (s), 1172 (w), 1135 (w), 1120 (w), 1093 (w), 1067 (w), 989 (s), 962 (w), 894 (w), 868 (w), 821 (m), 711 (m), 669 (w), 564 (m).

4.2.2. β-Chloroimine intermediate **(b)**

β-Chloroaldehyde **a** (2.166 g, 14.98 mmol) was dissolved in diethyl ether (20 mL) and cooled to 0 °C for 10 min. Activated 4 Å molecular sieves were added, followed by (2,6-$Me_2C_6H_3$)NH_2 (2.000 g, 16.50 mmol) diluted with diethyl ether (10 mL). The resulting solution slowly warmed to ambient temperature with stirring for 14 h. The solution was passed through a pad of Celite® and volatiles removed in vacuo to constant weight to yield a red liquid, which was used without further purification (3.56 g, 95.9%); ^{1}H NMR δ = 8.44 (s, 1H), 7.04 (d, $^{3}J_{HH}$ = 7.2 Hz, 2H), 6.92 (t, $^{3}J_{HH}$ = 7.2 Hz, 1H), 2.62–2.59 (m, 2H), 2.58–2.55 (m, 2H), 2.10 (s, 6H), 1.85–1.81 (m, 2H), 1.78–1.74 (m, 2H); ^{13}C{^{1}H} NMR δ = 161.8, 151.7, 142.6, 131.8, 128.2, 127.1, 123.8, 35.6, 25.8, 23.8, 21.8, 18.6; IR (neat) 3288 (w), 3007 (w), 2932 (s), 2858 (m), 2728 (w), 2356 (w), 2328 (w), 1918 (w), 1848 (w), 1690 (m), 1616 (s), 1588 (m), 1527 (w), 1472 (s), 1379 (w), 1355 (w), 1318 (w), 1272 (w), 1230 (m), 1193 (m), 1165 (w), 1128 (w), 1086 (m), 1035 (w), 988 (m), 914 (w), 895 (w), 877 (w), 844 (w), 825 (m), 765 (s), 732 (w), 719 (m), 663 (m).

4.2.3. 3IP^{Ar}

In the glovebox, two Schlenk tubes were charged with β-chloroimine **b** (0.372 g, 1.50 mmol) and lithium diphenylphosphide (0.346 g, 1.80 mmol). Toluene (30 mL) was added to each Schlenk tube and cooled to −78 °C for 10 min. The imine solution was added to the phosphide suspension and stirred for 14 h, slowly warming to ambient temperature. Volatiles were removed in vacuo and the crude product triturated with pentane (10 mL). The product was extracted with pentane (3 × 25 mL), filtered and dried in vacuo to give an off-white foamy solid (0.523 g, 87.7%); ^{1}H NMR δ = 9.05 (d, $^{4}J_{PH}$ = 9.0 Hz, 1H), 7.35–7.32 (m, 10H), 6.98 (d, $^{3}J_{HH}$ = 7.2 Hz, 2H), 6.88 (t, $^{3}J_{HH}$ = 7.2 Hz, 1H), 2.78–2.75 (m, 2H), 1.99–1.96 (m, 2H), 1.97 (s, 6H), 1.77–1.73 (m, 2H), 1.68–1.65 (m, 2H); ^{13}C{^{1}H} NMR δ = 163.0 (d, $^{3}J_{PC}$ = 41.2 Hz), 151.7, 147.3 (d, $^{2}J_{PC}$ = 18.2 Hz), 145.3 (d, $^{1}J_{PC}$ = 23.0 Hz), 136.3 (d, $^{1}J_{PC}$ = 11.1 Hz), 133.5 (d, $^{2}J_{PC}$ = 19.0 Hz), 128.8 (d, $^{3}J_{PC}$ = 4.5 Hz), 128.7, 128.1, 127.3, 123.6, 30.7 (d, $^{3}J_{PC}$ = 4.0 Hz), 26.6 (d, $^{2}J_{PC}$ = 5.7 Hz), 23.6, 22.2, 18.5; ^{31}P{^{1}H} NMR δ = −12.6; IR(nujol) 3068 (m), 3057 (m), 3016 (w), 2933 (m), 2860 (m), 2736 (w), 2674 (w), 2362 (w), 2279 (w), 1953 (w), 1880 (w), 1813 (w), 1776 (w), 1750 (w), 1657 (w), 1615 (s), 1589 (m), 1475 (m), 1434 (s), 1372 (w), 1351 (w), 1325 (w), 1304 (w), 1257 (m), 1221 (w), 1190 (m), 1159 (w), 1091 (s), 1065 (m), 1024 (s), 915 (w), 889 (w), 842 (m), 801 (s), 764 (m), 744 (s), 723 (m), 697 (s), 601 (w); $HRMS_{calc}$: 398.2038 for $C_{27}H_{29}NP$ $[M + H]^+$; $HRMS_{meas}$: 398.2041.

4.2.4. (3IP^{Ar})PdCl$_2$

A slurry of palladium(II) chloride (0.155 g, 0.876 mmol) in acetonitrile (30 mL) and **3IP^{Ar}** (0.383 g, 0.964 mmol) in methylene chloride (10 mL) were combined and allowed to stir at ambient temperature for 12 h. Solvent was removed in vacuo yielding a sticky orange solid which was triturated with pentane (2 × 5 mL) and washed with diethyl ether (2 × 10 mL). The solid was extracted with methylene chloride and precipitated using diethyl ether at −25 °C as a yellow powder (0.302 g, 60.0%). Single crystals suitable for an X-ray diffraction study were grown by slow evaporation of a concentrated chloroform solution; mp 194–196 °C; ^{1}H NMR δ = 7.73 (dd, $^{3}J_{PH}$ = 11.4 Hz, $^{3}J_{HH}$ = 7.8 Hz, 4H), 7.56 (t, $^{3}J_{HH}$ = 7.2 Hz, 2H), 7.48 (pseudo t, $^{3}J_{HH}$ = 7.8 Hz, $^{3}J_{HH}$ = 7.2 Hz, 4H), 7.46 (s, 1H), 7.04 (t, $^{3}J_{HH}$ = 7.8 Hz, 1H), 6.98 (d, $^{3}J_{HH}$ = 7.8 Hz, 2H), 2.58–2.56 (m, 2H), 2.10 (s, 6H), 1.90–1.88 (m, 2H), 1.84–1.81 (m, 2H), 1.73–1.70 (m, 2H); ^{13}C{^{1}H} NMR δ = 165.0 (d, $^{3}J_{PC}$ = 15.3 Hz), 151.7, 145.9 (d, $^{2}J_{PC}$ = 12.9 Hz), 133.7 (d, $^{2}J_{PC}$ = 10.8 Hz), 132.2 (d, $^{4}J_{PC}$ = 2.8 Hz), 131.5 (d, $^{1}J_{PC}$ = 37.2 Hz), 130.2, 129.3 (d, $^{3}J_{PC}$ = 11.7 Hz), 128.4, 127.4, 126.5 (d, $^{1}J_{PC}$ = 59.2 Hz), 32.8 (d, $^{2}J_{PC}$ = 9.8 Hz), 30.4, 22.5 (d, $^{3}J_{PC}$ = 4.2 Hz), 21.6, 19.4; ^{31}P{^{1}H} δ = 30.3; IR(nujol) 2955 (s), 2904 (s), 2862 (s), 2727 (w), 2664 (w), 1626 (w), 1580 (w), 1455 (s), 1372 (s), 1305 (w), 1258 (w), 1186 (w), 1144 (w), 1113 (m), 1092 (m), 1025 (w), 993 (w), 962 (w), 921 (w), 885 (w), 802 (w), 770 (m), 744 (m), 718 (m), 693 (m), 662 (m); Anal. Calcd for $C_{27}H_{28}Cl_2NPPd \cdot 2.5\ CH_2Cl_2$: C, 45.01; H, 4.23; N, 1.78. Found: C, 45.13; H, 4.06; N, 1.94.

4.2.5. (3IP^{Ar})Pd(allyl)Cl

In the glovebox, Schlenk flasks were charged separately with **3IP^{Ar}** (767 mg, 1.93 mmol) and $[Pd(allyl)Cl]_2$ (366 mg, 1.00 mmol). At room temperature, methylene chloride (10 mL) was added to each flask and the **3IP^{Ar}** solution slowly cannulated into the Pd suspension and stirred overnight. The deep orange solution was filtered, solvent removed in vacuo, and the resulting yellow solid washed with pentane (2 × 10 mL) to give a yellow powder (1.06 g, 94.6%); mp 84–87 °C; ^{1}H NMR δ = 8.81 (d, $^{4}J_{PH}$ = 3.6 Hz, 1H), 7.65–7.60 (m, 4H), 7.43–7.37 (m, 6H), 6.89 (d, $^{3}J_{HH}$ = 7.2 Hz, 2H), 6.82 (t, $^{3}J_{HH}$ = 7.2 Hz, 1H), 5.10 (pent, $^{3}J_{HH}$ = 10.2 Hz, 1H), 4.22 (v br s, 1H), 3.38 (v br s, 1H), 2.82 (v br s, 2H), 2.79–2.75 (m, 2H), 1.90–1.85 (m, 2H), 1.88 (s, 6H), 1.77–1.73 (m, 2H), 1.67–1.63 (m, 2H); ^{13}C{^{1}H} NMR δ = 171.1, 162.8 (d, $^{1}J_{PC}$ = 25.5 Hz), 152.0, 145.4 (d, $^{2}J_{PC}$ = 6.2 Hz), 138.8 (d, $^{1}J_{PC}$ = 28.4 Hz), 134.3 (d, $^{3}J_{CP}$ = 12.7 Hz), 130.8, 128.9 (d, $^{2}J_{PC}$ = 10.3 Hz), 127.9, 126.8, 124.0, 118.0 (d, $^{2}J_{CP}$ = 5.6 Hz), 78.8 (v br), 60.4 (v br), 32.2, 27.0 (d, $^{2}J_{PC}$ = 8.7 Hz), 23.2 (d, $^{3}J_{PC}$ = 5.3 Hz), 21.6, 18.4; ^{31}P{^{1}H} NMR δ = 19.1; IR(nujol) 3052 (w), 2925 (s), 2850 (s), 1613 (s), 1591 (m), 1464 (s), 1427 (s), 1375 (m), 1263 (w), 1196 (m), 1092 (s), 1017 (w), 846 (w), 801 (w), 749 (s), 697 (s); $HRMS_{calc}$: 544.1385 for $C_{30}H_{33}NPPd^+$ $[M - Cl^-]^+$; $HRMS_{meas}$: 544.1375.

4.2.6. [(3IP^{Ar})Pd(allyl)]OTf

In the glovebox, a Schlenk flask was charged with **(3IP^{Ar})Pd(allyl)Cl** (565 mg, 0.973 mmol) and silver triflate (257 mg, 1.00 mmol). In the absence of light, methylene chloride (15 mL) was added and the resulting suspension stirred at room temperature overnight. The reaction mixture was filtered to give a yellow/orange solution. Solvent was removed in vacuo and the resulting yellow solid washed with pentane (2 × 10 mL) to afford a microcrystalline yellow solid (593 mg, 87.9%); mp 103–107 °C; ^{1}H NMR [47] δ = 7.70 (s, 1H), 7.60–7.48 (m, 8H), 7.46–7.41 (m, 2H), 7.12 (broad s, 3H), 5.78–5.71 (m, 1H), 3.58 (t, $^{3}J_{PH}$ = 6.6 Hz, $^{3}J_{HH}$ = 6.6 Hz, 1H), 3.50 (dd, $^{3}J_{PH}$ = 14.4 Hz, $^{3}J_{HH}$ = 9.6 Hz, 1H), 3.43 (d, $^{3}J_{HH}$ = 6.6 Hz, 1H), 2.76 (d, $^{3}J_{HH}$ = 12.6 Hz, 1H), 2.73–2.62 (m, 2H), 2.06 (s, 3H), 2.04–2.02 (m, 1H), 1.99–1.97 (m, 1H), 1.95 (s, 3H), 1.87–1.83 (m, 1H), 1.81–1.78 (m, 1H), 1.77–1.71 (m, 2H); ^{13}C{^{1}H} NMR [47] δ = 168.0 (d, $^{3}J_{PC}$ = 10.8 Hz), 154.9, 146.2 (d, $^{2}J_{PC}$ = 12.4 Hz), 133.2 (d, $^{2}J_{PC}$ = 13.3 Hz), 133.0, 132.9 (d, $^{2}J_{PC}$ = 13.0 Hz), 132.2 (d, $^{4}J_{PC}$ = 2.1 Hz), 132.1 (d, $^{4}J_{PC}$ = 2.1 Hz), 130.0 (d, $^{3}J_{PC}$ = 10.9 Hz), 129.9 (d, $^{3}J_{PC}$ = 10.9 Hz), 128.9 (d,

$^1J_{PC}$ = 19.6 Hz), 128.3 (d, $^1J_{PC}$ = 48.0 Hz), 127.8 (d, $^1J_{PC}$ = 46.3 Hz), 127.3, 126.9, 123.6 (d, $^2J_{PC}$ = 6.0 Hz), 84.5 (d, $^2J_{PC}$ = 28.8 Hz), 55.8 (d, $^2J_{PC}$ = 4.4 Hz), 33.7 (d, $^3J_{PC}$ = 10.3 Hz), 30.1, 22.3 (d, $^3J_{PC}$ = 4.1 Hz), 21.6, 18.5 (d, $^2J_{PC}$ = 20.1 Hz); $^{31}P\{^1H\}$ NMR δ = 25.2; ^{19}F NMR δ = −78.3; IR(nujol) 3050 (w), 2926 (s), 2852 (s), 2727 (w), 2678 (w), 2293 (w), 1976 (w), 1908 (w), 1834 (w), 1629 (m), 1579 (m), 1461 (s), 1437 (s), 1381 (m), 1269 (s), 1225 (s), 1194 (m), 1145 (s), 1095 (s), 1064 (m), 1027 (s), 909 (m), 779 (s), 754 (s), 698 (s), 636 (s); $HRMS_{calc}$: 544.1385 for $C_{30}H_{33}NPPd^+$ $[M]^+$; $HRMS_{meas}$: 544.1375; Anal. Calcd. for $C_{31}H_{33}F_3NO_3PPdS \cdot ½\ CH_2Cl_2$: C, 51.37; H, 4.65; N, 1.90. Found: C, 51.36; H, 4.30; N, 1.99.

4.3. Catalysis

4.3.1. General procedure for the Pd catalyzed hydroamination of dienes

All manipulations were performed in an inert atmosphere glovebox (N_2). The Pd catalyst (10.2 mg, 0.0147 mmol, 5 mol%), C_6D_6 (0.5 mL), amine (0.32 mmol), and lastly diene (0.32 mmol) were added to a J-Young NMR tube that was subsequently sealed. Upon addition of the amine, the pale yellow suspension rapidly turned to a deep red solution. The reaction progress was monitored by ^1H NMR until completion, as assessed by the complete disappearance of diene. Product allyl amines were isolated as follows: the crude reaction mixture was loaded onto a short column of Al_2O_3 (0.5 inches) and eluted with toluene. The product band was subsequently reduced under rotary evaporation at 35 °C to constant mass. Representative examples: **2a** (45 mg isolated; 91%); **3a** (39 mg isolated; 72%).

4.3.2. 1,2-Diene addition products

N-(3-Methyl-2-buten-1-yl)-morpholine (**2a**) [33,48], *N*-(3-methyl-2-buten-1-yl)-piperidine (**2d**) [48], *N*-(3-methyl-2-buten-1-yl)-diethylamine (**2f**) [33,49], *N*-(3-methyl-2-buten-1-yl)-dibenzylamine (**2i**) [33], *N*-(3-methyl-2-buten-1-yl)-1,2,3,4-tetrahydroisoquinoline (**2j**) [33,48], *N*-(3-methyl-2-buten-1-yl)-indoline (**2k**) [33] and *N*-(3-methyl-2-buten-1-yl)-1,2,3,4-tetrahydroquinoline (**2m**) [33], were identified by comparison to published NMR data. Compounds listed below with references represent previously reported species with no spectral data or from difficult to access journals.

4.3.2.1. N-(3-Methyl-2-buten-1-yl),N′-methyl-piperazine ***(2b)***. ^1H NMR δ = 5.07 (t, $^3J_{HH}$ = 7.2 Hz, 1H), 2.76 (d, $^3J_{HH}$ = 7.2 Hz, 2H), 2.28–2.24 (broad m, 8H), 2.09 (s, 3H), 1.54 (s, 3H), 1.45 (s, 3H); $^{13}C\{^1H\}$ NMR δ = 134.9, 120.8, 55.8, 55.0, 52.9, 45.8, 25.7, 17.8; $HRMS_{calc}$: 169.1705 for $C_{10}H_{21}N_2$ $[M + H]^+$; $HRMS_{meas}$: 169.1707.

4.3.2.2. N-(3-Methyl-2-buten-1-yl)-thiomorpholine ***(2c)***. ^1H NMR (C_6D_6) δ = 5.21 (t, $^3J_{HH}$ = 7.2 Hz, 1H), 2.74 (d, $^3J_{HH}$ = 7.2 Hz, 2H), 2.45–2.37 (broad m, 8H), 1.55 (s, 3H), 1.41 (s, 3H); $^{13}C\{^1H\}$ NMR (C_6D_6) δ = 135.2, 122.6, 57.6, 55.6, 28.8, 26.3, 18.4; $HRMS_{calc}$: 172.1160 for $C_9H_{18}NS$ $[M + H]^+$; $HRMS_{meas}$: 172.1165.

4.3.2.3. N-(3-Methyl-2-buten-1-yl)-pyrrolidine ***(2e)*** *[50].* ^1H NMR δ = 5.28 (t, $^3J_{HH}$ = 6.8 Hz, 1H), 3.03 (d, $^3J_{HH}$ = 6.8 Hz, 2H), 2.49–2.35 (m, 4H), 1.85–1.64 (m, 4H), 1.69 (s, 3H), 1.62 (s, 3H); $^{13}C\{^1H\}$ NMR δ = 134.1, 122.2, 54.2, 53.7, 26.1, 23.6, 18.2.

4.3.2.4. N-(3-Methyl-2-buten-1-yl)-di-n-butylamine ***(2g)*** *[51].* ^1H NMR δ = 5.22 (t, $^3J_{HH}$ = 6.8 Hz, 1H), 3.00 (d, $^3J_{HH}$ = 6.8 Hz, 2H), 2.36 (m, 4H), 1.70 (s, 3H), 1.61 (s, 3H), 1.44–1.38 (m, 4H), 1.33–1.22 (m, 4H), 0.88 (t, $^3J_{HH}$ = 7.6 Hz, 6H); $^{13}C\{^1H\}$ NMR δ = 134.1, 122.3, 53.8, 51.9, 29.5, 26.1, 21.0, 18.2, 14.3; $HRMS_{calc}$: 198.2222 for $C_{13}H_{28}N$ $[M + H]^+$; $HRMS_{meas}$: 198.2227.

4.3.2.5. N-(3-Methyl-2-buten-1-yl)-N-methyl-n-butylamine ***(2h)***. ^1H NMR δ = 5.30 (t, $^3J_{HH}$ = 6.6 Hz, 1H), 2.96 (d, $^3J_{HH}$ = 6.6 Hz, 2H), 2.35 (t, $^3J_{HH}$ = 7.2 Hz, 2H), 2.22 (s, 3H), 1.77 (s, 3H), 1.68 (s, 3H), 1.43–1.26 (m, 2H), 1.36 (m, 2H), 0.96 (t, $^3J_{HH}$ = 7.2 Hz, 3H); $^{13}C\{^1H\}$ NMR δ = 134.6, 122.0, 57.4, 55.5, 42.2, 29.8, 26.0, 20.9, 18.0, 14.2; $HRMS_{calc}$: 156.1752 for $C_{10}H_{22}N$ $[M + H]^+$; $HRMS_{meas}$: 156.1754.

4.3.2.6. N-(3-Methyl-2-buten-1-yl)-2-methylindoline ***(2l)***. ^1H NMR (C_6D_6) δ = 7.14 (t, $^3J_{HH}$ = 7.2 Hz, 1H), 7.03 (d, $^3J_{HH}$ = 7.2 Hz, 1H), 6.76 (t, $^3J_{HH}$ = 7.2 Hz, 1H), 6.51 (d, $^3J_{HH}$ = 7.2 Hz, 1H), 5.29–5.25 (m, 1H), 3.66 (dd, $^2J_{HH}$ = 16.2 Hz, $^3J_{HH}$ = 4.2 Hz, 1H), 3.59 (dd, $^2J_{HH}$ = 16.2 Hz, $^3J_{HH}$ = 7.8 Hz, 1H), 3.53–3.45 (m, 1H), 2.84 (dd, $^2J_{HH}$ = 15.0 Hz, $^3J_{HH}$ = 8.4 Hz, 1H), 2.42 (dd, $^2J_{HH}$ = 15.0 Hz, $^3J_{HH}$ = 10.2 Hz, 1H), 1.54 (s, 3H), 1.51 (s, 3H), 1.09 (d, $^3J_{HH}$ = 6.0 Hz, 3H); $^{13}C\{^1H\}$ NMR (C_6D_6) δ = 153.0, 134.0, 129.3, 127.8, 124.5, 121.4, 117.9, 107.6, 59.5, 43.9, 37.6, 25.7, 19.3, 17.9; $HRMS_{calc}$: 202.1596 for $C_{14}H_{20}N$ $[M + H]^+$; $HRMS_{meas}$: 202.1590.

4.3.3. 1,3-Diene addition products

N-(2,3-Dimethyl-2-buten-1-yl)-piperidine ***(3d)*** [49] and N-(2,3-dimethyl-2-buten-1-yl)-diethylamine **(3f)** [49] were identified by comparison to published NMR data. Compounds listed below with references represent previously reported species with no spectral data or from difficult to access journals.

4.3.3.1. N-(2,3-Dimethyl-2-buten-1-yl)-morpholine ***(3a)*** *[52].* ^1H NMR (C_6D_6) δ = 3.55 (t, $^3J_{HH}$ = 4.4 Hz, 4H), 2.73 (s, 2H), 2.15 (t, $^3J_{HH}$ = 4.4 Hz, 4H), 1.69 (s, 3H), 1.56 (broad s, 6H); $^{13}C\{^1H\}$ NMR (C_6D_6) δ = 128.9, 125.5, 67.7, 61.9, 54.3, 21.4, 20.7, 18.1.

4.3.3.2. N-(2,3-Dimethyl-2-buten-1-yl),N′-methyl-piperazine ***(3b)***. ^1H NMR δ = 2.86 (s, 2H), 2.61–2.15 (broad s, 8H), 2.23 (s, 3H), 1.66–1.62 (overlapping s, 9H); $^{13}C\{^1H\}$ NMR δ = 128.5, 125.0, 61.0, 55.5, 53.1, 46.2, 21.1, 20.4, 17.8; $HRMS_{calc}$: 183.1861 for $C_{11}H_{23}N_2$ $[M + H]^+$; $HRMS_{meas}$: 183.1869.

4.3.3.3. N-(2,3-Dimethyl-2-buten-1-yl)-thiomorpholine ***(3c)***. ^1H NMR δ = 2.89 (s, 2H), 2.64–2.58 (m, 8H), 1.67 (s, 3H), 1.66 (s, 3H), 1.65 (s, 3H); $^{13}C\{^1H\}$ NMR δ = 128.9, 124.9, 61.8, 54.9, 28.4, 21.2, 20.4, 17.6; $HRMS_{calc}$: 186.1316 for $C_{10}H_{20}NS$ $[M + H]^+$; $HRMS_{meas}$: 186.1323.

4.3.3.4. N-(2,3-Dimethyl-2-buten-1-yl)-pyrrolidine ***(3e)***. ^1H NMR δ = 3.03 (s, 2H), 2.46–2.42 (m, 4H), 1.76–1.66 (m, 10H), 1.66 (s, 3H); $^{13}C\{^1H\}$ NMR δ = 128.4, 126.3, 58.9, 54.4, 23.7, 21.1, 20.5, 18.1; $HRMS_{calc}$: 154.1596 for $C_{10}H_{20}N$ $[M + H]^+$; $HRMS_{meas}$: 154.1592.

4.3.3.5. N-(2,3-Dimethyl-2-buten-1-yl)-di-n-butylamine ***(3g)***. ^1H NMR δ = 2.89 (s, 2H), 2.29 (t, $^3J_{HH}$ = 7.2 Hz, 4H), 1.68 (s, 3H), 1.66 (broad s, 6H), 1.43–1.33 (m, 4H), 1.32–1.23 (m, 4H), 0.88 (t, $^3J_{HH}$ = 7.2 Hz, 6H); $^{13}C\{^1H\}$ NMR δ = 127.2, 126.8, 57.1, 53.6, 29.5, 21.2, 20.9, 20.4, 17.6, 14.3; $HRMS_{calc}$: 212.2378 for $C_{14}H_{30}N$ $[M + H]^+$; $HRMS_{meas}$: 212.2373.

4.3.3.6. N-(2,3-Dimethyl-2-buten-1-yl)-1,2,3,4-tetrahydroisoquinoline ***(3j)***. ^1H NMR δ = 7.16–7.12 (m, 3H). 7.07–7.03 (m, 1H), 3.61 (s, 2H), 3.13, (s, 2H), 2.91 (t, $^3J_{HH}$ = 4.8 Hz, 2H), 2.69 (t, $^3J_{HH}$ = 4.8 Hz, 2H), 1.79 (broad s, 6H), 1.77 (s, 3H); $^{13}C\{^1H\}$ NMR δ = 135.6, 134.9, 128.8, 128.6, 126.8, 126.1, 125.6, 125.3, 60.9, 56.4, 50.4, 29.5, 21.2, 20.5, 17.8; $HRMS_{calc}$: 216.1752 for $C_{15}H_{22}N$ $[M + H]^+$; $HRMS_{meas}$: 216.1759.

4.3.3.7. N-(2,3-Dimethyl-2-buten-1-yl)-indoline ***(3k)***. ^1H NMR δ = 7.15–7.06 (m, 2H), 6.71–6.66 (m, 1H), 6.60–6.54 (m, 1H), 3.69 (s, 2H), 3.28 (t, $^3J_{HH}$ = 8.4 Hz, 2H), 2.97 (t, $^3J_{HH}$ = 8.4 Hz, 2H), 1.83 (s, 3H), 1.79 (broad s, 6H); $^{13}C\{^1H\}$ NMR δ = 153.4, 130.3, 127.5, 124.5,

Table 6
Crystal data and collection parameters.

Compound	$(3IP^{Ar})PdCl_2$	$[(3IP^{Ar})Pd(allyl)]OTf$
Formula	$C_{27}H_{28}Cl_2NPPd \cdot 2\ CHCl_3$	$C_{31}H_{33}F_3NO_3PPdS \cdot ½\ C_4H_8O$
Fw	813.51	730.07
space group	$P2_12_12_1$ (#19)	$C2/c$ (#15)
temperature (K)	150(2)	140(2)
a (Å)	11.3505(8)	36.441(2)
b (Å)	14.518(1)	8.9994(5)
c (Å)	20.324(1)	20.505(1)
α (deg)	90.000	90.000
β (deg)	90.000	103.822(1)
γ (deg)	90.000	90.000
V (Å^3)	3349.1(4)	6529.7(6)
Z	4	8
density$_{calc}$ (g/cm^3)	1.613	1.485
Diffractometer	Siemens SMART	Siemens SMART
Radiation	Mo K$_\alpha$ (λ = 0.71073 Å)	Mo K$_\alpha$ (λ = 0.71073 Å)
Monochromator	Graphite	Graphite
Detector	CCD area detector	CCD area detector
scan type, width	ω, 0.3°	ω, 0.3°
scan speed	20 s/frame	20 s/frame
no. of reflns measd	Hemisphere	Hemisphere
2θ range (deg)	3.44–66.78	2.30–61.22
cryst dimens (mm)	0.28 × 0.16 × 0.10	0.28 × 0.22 × 0.10
no. of reflns measd	47874	41520
no. of unique reflns	12106	10027
no. of obs. ($I > 2\sigma(I)$)	10783	8986
R_{int}	0.0661	0.0388
no. of params	361	428
R, R_w, R_{all}	0.0756, 0.1334, 0.0881	0.0411, 0.1104, 0.0453
GOF	1.193	1.018

122.1, 120.8, 117.3, 106.9, 53.2, 51.9, 28.6, 21.2, 20.4, 17.2; HRMS$_{calc}$: 202.1596 for $C_{14}H_{20}N$ $[M + H]^+$; HRMS$_{meas}$: 202.1590.

4.4. Crystallography

Summaries of crystal data and collection parameters for crystal structures of **$(3IP^{Ar})PdCl_2$** and **$[(3IP^{Ar})Pd(allyl)]OTf$** are provided in Table 6. Detailed descriptions of data collection, as well as data solution, are provided below. ORTEP diagrams were generated with the ORTEP-3 software package [53]. For each sample, a suitable crystal was mounted on a pulled glass fiber using Paratone-N hydrocarbon oil. The crystal was transferred to a Siemens SMART [54] diffractometer with a CCD area detector, centered in the X-ray beam, and cooled to the indicated temperature using a nitrogen-flow low-temperature apparatus that had been previously calibrated by a thermocouple placed at the same position as the crystal. An arbitrary hemisphere of data was collected using 0.3° ω scans, and the data were integrated by the program SAINT [55]. The final unit cell parameters were determined by a least-squares refinement of the reflections with $I > 10\sigma(I)$. Data analysis using Siemens XPREP [56] and the successful solution and refinement of the structure determined the space group. An empirical absorption correction was applied using SADABS [57]. Equivalent reflections were averaged, and the structures were solved by direct methods using the SHELXTL software package [58]. All non-hydrogen atoms were refined anisotropically, and hydrogen atoms were included as fixed atoms but not refined.

4.4.1. $(3IP^{Ar})PdCl_2$

X-ray quality crystals were grown by slow evaporation of a saturated solution in chloroform at ambient temperature. The final cycle of full-matrix least-squares refinement was based on 10783 observed reflections and 361 variable parameters and converged yielding final residuals: $R = 0.0756$, $R_{all} = 0.0881$, and GOF = 1.193.

4.4.2. $[(3IP^{Ar})Pd(allyl)]OTf$

X-ray quality crystals were grown by slow diffusion of pentane into a THF solution of the complex at ambient temperature. In the final model, the allyl group was found to be disordered in a 4:1 ratio of *cis* and *trans* isomers, while the 3- and 4-carbons of the cyclohexenyl unit were disordered in a 1:1 ratio of two boat-like conformations. The final cycle of full-matrix least-squares refinement was based on 8986 observed reflections and 428 variable parameters and converged yielding final residuals: $R = 0.0411$, $R_{all} = 0.0453$, and GOF = 1.018.

Acknowledgements

This material is based upon work supported by the National Science Foundation under CHE-0841611.

Appendix A. Supplementary material

CCDC 783884 (**$(3IP^{Ar})PdCl_2$**) and CCDC 783885 (**$[(3IP^{Ar})Pd(allyl)]OTf$**) contain the supplementary crystallographic data for this paper. These data can be obtained free of charge from The Cambridge Crystallographic Data Centre via www.ccdc.cam.ac.uk/data_request/cif.

References

[1] G.R. Maxwell, Synthetic Nitrogen Products: A Practical Guide to the Products and Processes. Kluwer Academic /Plenum Publishers, New York, 2004.
[2] S.A. Lawrence, Amines: Synthesis, Properties, and Applications. Cambridge University Press, New York, 2004.
[3] T.E. Muller, K.C. Hultzsch, M. Yus, F. Foubelo, M. Tada, Chem. Rev. 108 (2008) 3795–3892.
[4] U. Dzhemilev, G. Tolstikov, R. Khusnutdinov, Russ. J. Org. Chem. 45 (2009) 957–987.
[5] R.A. Widenhoefer, X.Q. Han, Eur. J. Org. Chem. (2006) 4555–4563.
[6] F. Pohlki, S. Doye, Chem. Soc. Rev. 32 (2003) 104–114.
[7] S. Hong, T.J. Marks, Acc. Chem. Res. 37 (2004) 673–686.
[8] J.F. Hartwig, Pure Appl. Chem. 76 (2004) 507–516.
[9] I. Aillaud, J. Collin, J. Hannedouche, E. Schulz, Dalton Trans. (2007) 5105–5118.
[10] Y. Yamamoto, U. Radhakrishnan, Chem. Soc. Rev. 28 (1999) 199–207.
[11] C.F. Bender, R.A. Widenhoefer, J. Am. Chem. Soc. 127 (2005) 1070–1071.
[12] E.B. Bauer, G.T.S. Andavan, T.K. Hollis, R.J. Rubio, J. Cho, G.R. Kuchenbeiser, T.R. Helgert, C.S. Letko, F.S. Tham, Org. Lett. 10 (2008) 1175–1178.
[13] K.D. Hesp, M. Stradiotto, Org. Lett. 11 (2009) 1449–1452.
[14] K.D. Hesp, S. Tobisch, M. Stradiotto, J. Am. Chem. Soc. 132 (2010) 413–426.
[15] H. Ohmiya, T. Moriya, M. Sawamura, Org. Lett. 11 (2009) 2145–2147.
[16] C.F. Bender, W.B. Hudson, R.A. Widenhoefer, Organometallics 27 (2008) 2356–2358.
[17] Z. Liu, J.F. Hartwig, J. Am. Chem. Soc. 130 (2008) 1570–1571.
[18] X.Q. Shen, S.L. Buchwald, Angew. Chem. Int. Ed. 49 (2010) 564–567.
[19] Z.Y. Han, H. Xiao, X.H. Chen, L.Z. Gong, J. Am. Chem. Soc. 131 (2009) 9182–9183.
[20] J.M. Carney, P.J. Donoghue, W.M. Wuest, O. Wiest, P. Helquist, Org. Lett. 10 (2008) 3903–3906.
[21] S.R. Beeren, S.L. Dabb, B.A. Messerle, J. Organomet. Chem. 694 (2009) 309–312.
[22] S.L. Dabb, J.H.H. Ho, R. Hodgson, B.A. Messerle, J. Wagler, Dalton Trans. (2009) 634–642.
[23] K. Ogata, T. Nagaya, S. Fukuzawa, J. Organomet. Chem. 695 (2010) 1675–1681.
[24] M. Dochnahl, K. Lohnwitz, A. Luhl, J.-W. Pissarek, M. Biyikal, P.W. Roesky, S. Blechert, Organometallics 29 (2010) 2637–2645.
[25] F.E. Michael, B.M. Cochran, J. Am. Chem. Soc. 128 (2006) 4246–4247.
[26] L.M. Lutete, I. Kadota, Y. Yamamoto, J. Am. Chem. Soc. 126 (2004) 1622–1623.
[27] M. Beller, O.R. Thiel, H. Trauthwein, C.G. Hartung, Chem. Eur. J. 6 (2000) 2513–2522.
[28] X.W. Li, A.R. Chianese, T. Vogel, R.H. Crabtree, Org. Lett. 7 (2005) 5437–5440.
[29] C. Brouwer, C. He, Angew. Chem. Int. Ed. 45 (2006) 1744–1747.
[30] R.L. LaLonde, B.D. Sherry, E.J. Kang, F.D. Toste, J. Am. Chem. Soc. 129 (2007) 2452–2453.
[31] N. Nishina, Y. Yamamoto, Angew. Chem. Int. Ed. 45 (2006) 3314–3317.
[32] S.F. Qiu, Y.Y. Wei, G.S. Liu, Chem. Eur. J. 15 (2009) 2751–2754.
[33] X.M. Zeng, M. Soleilhavoup, G. Bertrand, Org. Lett. 11 (2009) 3166–3169.
[34] V. Lavallo, G.D. Frey, B. Donnadieu, M. Soleilhavoup, G. Bertrand, Angew. Chem. Int. Ed. 47 (2008) 5224–5228.
[35] A.N. Duncan, R.A. Widenhoefer, Synlett (2010) 419–422.
[36] R.E. Kinder, Z. Zhang, R.A. Widenhoefer, Org. Lett. 10 (2008) 3157–3159.

[37] Z.B. Zhang, C.F. Bender, R.A. Widenhoefer, J. Am. Chem. Soc. 129 (2007) 14148–14149.
[38] Z.B. Zhang, C.F. Bender, R.A. Widenhoefer, Org. Lett. 9 (2007) 2887–2889.
[39] H. Li, R.A. Widenhoefer, Org. Lett. 11 (2009) 2671–2674.
[40] A.R. Shaffer, J.A.R. Schmidt, Organometallics 28 (2009) 2494–2504.
[41] A.R. Shaffer, J.A.R. Schmidt, Organometallics 27 (2008) 1259–1266.
[42] K.L. Toups, R.A. Widenhoefer, Chem. Commun. 46 (2010) 1712–1714.
[43] L. Besson, J. Gore, B. Gazes, Tetrahedron Lett. 36 (1995) 3857–3860.
[44] N.D. Clement, L. Routaboul, A. Grotevendt, R. Jackstell, M. Beller, Chem. Eur. J. 14 (2008) 7408–7420.
[45] T. Minami, H. Okamoto, S. Ikeda, R. Tanaka, F. Ozawa, M. Yoshifuji, Angew. Chem. Int. Ed. 40 (2001) 4501–4503.
[46] W.R. Benson, A.E. Pohland, J. Org. Chem. 30 (1965) 1126–1129.
[47] For **[(3IP^{Ar})Pd(allyl)]OTf**, the ^{1}H NMR spectrum shows hindered rotation of the 2,6-$Me_2C_6H_3$ group on the NMR timescale, while this group rotates to equilibrate opposite sides on the ^{13}C NMR timescale.
[48] I.D.G. Watson, A.K. Yudin, J. Am. Chem. Soc. 127 (2005) 17516–17529.
[49] R.W. Armbruster, M.M. Morgan, J.L. Schmidt, C.M. Lau, R.M. Riley, D.L. Zabrowski, H.A. Dieck, Organometallics 5 (1986) 234–237.
[50] D. Cavalla, S. Warren, Tetrahedron Lett. 23 (1982) 4505–4508.
[51] O.A. Kazantsev, K.V. Shirshin, S.M. Danov, G.N. Afonshin, Zh. Org. Khim. 31 (1995) 334–337.
[52] U.M. Dzhemilev, A.Z. Yakupova, S.K. Minsker, G.A. Tolstikov, Zh. Org. Khim. 15 (1979) 1164–1169.
[53] L.J. Farrugia, J. Appl. Crystallogr. 30 (1997) 565.
[54] SMART: Area-Detector Software Package, v5.625. Bruker AXS, Inc., Madison, WI, 1997–2001.
[55] SAINT: SAX Area-Detector Integration Program, V6.22. Bruker AXS, Inc., Madison, WI, 1997–2001.
[56] XPREP: Reciprocal Space Exploration Program, V6.12. Bruker AXS, Inc., Madison, WI, 2001.
[57] SADABS: Bruker/Siemens Area Detector Absorption Program, V2.03. Bruker AXS, Inc., Madison, WI, 2001.
[58] SHELXL-97: Structure Solution Program, V6.10. Bruker AXS, Inc., Madison, WI, 2000.